THE STRUCTURES OF THE MINERALS OF THE DESCLOIZITE AND ADELITE GROUPS: II—PYROBELONITE

D. M. DONALDSON[1] AND W. H. BARNES, *Division of Physics, National Research Council, Ottawa, Canada.*

ABSTRACT

The structure of pyrobelonite, $PbMn(VO_4)(OH)$, has been established by two-dimensional Patterson, Fourier, and difference methods applied independently to each of the three principal zones. The coordination of oxygen around vanadium is tetrahedral; it is octahedral around manganese, and sevenfold around lead. Interatomic distances are given. The accuracy of the results is discussed in terms of the standard deviations of atomic positions and of interatomic distances. The close structural relationship of pyrobelonite to descloizite is confirmed.

INTRODUCTION

In continuation of a series of studies of the minerals of the descloizite and adelite groups (Barnes & Qurashi, 1952; Qurashi & Barnes, 1954), the structure of pyrobelonite, $PbMn(VO_4)(OH)$, has now been determined.

Both Strunz (1939) and Richmond (1940) are in agreement on the close structural relationship that must exist between pyrobelonite and descloizite, which is strikingly demonstrated by precession photographs of the three principal zones of each (see Qurashi & Barnes, 1954, Fig. 1). Interpretation of the original analytical results of Mauzelius (see Flink, 1919), however, has given rise to slight variations in the formula proposed for pyrobelonite, depending on the significance attached to the reported Mn:Pb ratio of 35:22. Thus Strunz (1939) gives it as $MnPb(VO_4)(OH)$ in his *Abstract* (p. 496) and *Summary* (p. 505), and as Mn (Pb, Mn) $(VO_4)(OH)$, to indicate replacement of some of the lead by manganese, in that section of his paper devoted especially to pyrobelonite (p. 502). On the other hand, Richmond expresses it as $(Mn, Pb)_2(VO_4)(OH)$, rounding off the Mn:Pb ratio to 5:3 in one place (p. 460) and 3:2 (perhaps a typographical error) in another (p. 477). In the latest edition of Dana's *System of Mineralogy* (1951) it is acknowledged that, if the observed Mn:Pb ratio (Flink, 1919) is real, "Mn may in part be in substitution for Pb, the formula then being $Mn(Pb, Mn)(VO_4)(OH)$," but the conclusion is reached that "the departure from the 1:1 ratio of Mn:Pb probably is due to analytical error" and the formula accepted, therefore

[1] National Research Laboratories Postdoctorate Fellow, now I.C.I. Fellow, The University, Edinburgh, Scotland.

is $MnPb(VO_4)(OH)$.* This has been employed successfully throughout the present structure investigation.

Experimental, and Crystal Data

The experimental data were obtained by means of Weissenberg and precession photographs (MoK_α radiation, $\lambda = 0.7107$ Å) of two crystals from Långban, Sweden (Harvard No. 94831) having dimensions $200 \times 50 \times 40\mu$ and $88 \times 50 \times 50\mu$, respectively.

Pyrobelonite is orthorhombic, space group *Pnma* (D_{2h}^{16}) or *Pn2a* (C_{2v}^{9}), with $a = 7.66_3$, $b = 6.19_1$, $c = 9.52_2$ Å (see Barnes & Qurashi, 1952). There are 4[$PbMn(VO_4)(OH)$] per cell and the calculated density is 5.79 gm. per ml. The observed density given by Hintze (1933), quoting Flink (1919), however, is only 5.377, and, if a Mn:Pb ratio of 5:3 were correct, the calculated value would be 5.23 gm. per ml. (although Richmond, 1940, gives it as 5.39). Apart from the two small crystals employed for the diffraction photographs, only one other from the Harvard 94831 specimen was available for the present investigation, but it had a mass of ~6 mg. Although this is too small for very accurate measurements with the Berman balance (Berman, 1939; Fairbairn & Sheppard, 1945), a value of 5.58 gm. per ml. (mean of ten determinations) was obtained for the density at 23° C., using carbon tetrachloride as the displacement liquid. The surface of the crystal was irregular, there were a few firmly-attached small fragments of other materials, and, owing to the virtual opacity it was not possible to estimate the degree of homogeneity of the crystal, so that the observed density probably is low rather than high. Crystals from another Långban specimen (U. S. National Museum No. 94601), freed from adhering matrix, were too small, and not sufficiently numerous, for a direct density determination, nor could any useful results be obtained by means of Cargille "heavy liquids." The question of the significance, if any, to be attached to the difference between the calculated and observed densities in relation to the possible substitution of managanese for lead will be mentioned later in the discussion.

Intensities were estimated visually from the precession and Weissenberg photographs using multiple exposure and multiple film techniques, respectively. The usual corrections for Lorentz and polarization factors were applied. For ease in the calculation of absorption corrections, the first crystal ($200 \times 50 \times 40\mu$), from which the $h0l$ reflection intensities were obtained, was treated as a cylinder, and the second, which was employed for the $\{hk0\}$ and $\{0kl\}$ zones, was considered as a sphere of vol-

* $PbMn(VO_4)(OH)$ is preferred for uniformity with descloizite, $Pb(Zn, Cu)(VO_4)(OH)$, and conichalcite, $CaCu(AsO_4)(OH)$ because the Pb in pyrobelonite and in descloizite, and the Ca in conichalcite, occupy corresponding sites in the structures of the three minerals.

ume $88\times50\times50\mu^3$. This has the advantage of making the absorption corrections, in all three zones, functions of sin θ (Bradley, 1935; Evans & Ekstein, 1952). The deviations from the true values should be small because of the comparative regularity of shape of the crystals and of their small size. The absorption coefficient for MoK_α ($\lambda=0.7107$ Å) is 474 per cm.

Analysis of the Structure

Because of the close similarity between corresponding reciprocal lattice nets of pyrobelonite and descloizite (Barnes & Qurashi, 1952; Qurashi & Barnes, 1954), the Pb, Mn and V atoms of pyrobelonite could justifiably have been assigned the parameters established for Pb, Zn, and V, respectively, in descloizite as a prelude to refinement of the pyrobelonite structure. It was decided, however, to carry out the present study as independently as possible of the descloizite results. Furthermore, one of the principal objects was to determine the coordinates of the oxygen atoms with the highest accuracy warranted by two-dimensional analysis of the data. Hence the three principal zones of pyrobelonite have been analysed separately and each has been refined without averaging the coordinates or correction factors (such as the temperature factor) among the three zones. This method provides a means for direct comparison of coordinates obtained independently for each of two separate zones.

The {h0l} Zone

Of 130 possible reflections in the range $\sin\theta/\lambda\leqq0.75$, 92 were observed, together with 8 outside this range. The (010) Patterson map was computed using all these observed reflections, and is reproduced in Fig. 1A. From an analysis of the peaks due to Pb-Pb, Pb-Mn, and Pb-V vectors, x and z coordinates for the metal atoms were obtained. Since the atomic numbers of Mn and V differ so slightly, it was impossible to distinguish between the positions occupied by the manganese and by the vanadium atoms. In this one instance, therefore, the descloizite structure was taken as a guide and the vanadium atoms in pyrobelonite were placed in the positions which corresponded most closely with those occupied by vanadium in descloizite. Structure factors were calculated* with these metal-atom coordinates and a Fourier synthesis was carried out. The (010) Fourier map is shown in Fig. 1B where it will be seen that the metal atoms are clearly resolved but only slight indications of the oxygen-atom positions appear.

* No choice between the alternative space groups (*Pnma* and *Pn2a*) was necessary at this stage because the equivalent positions and structure factor equations are the same for the {*h*0*l*} zone.

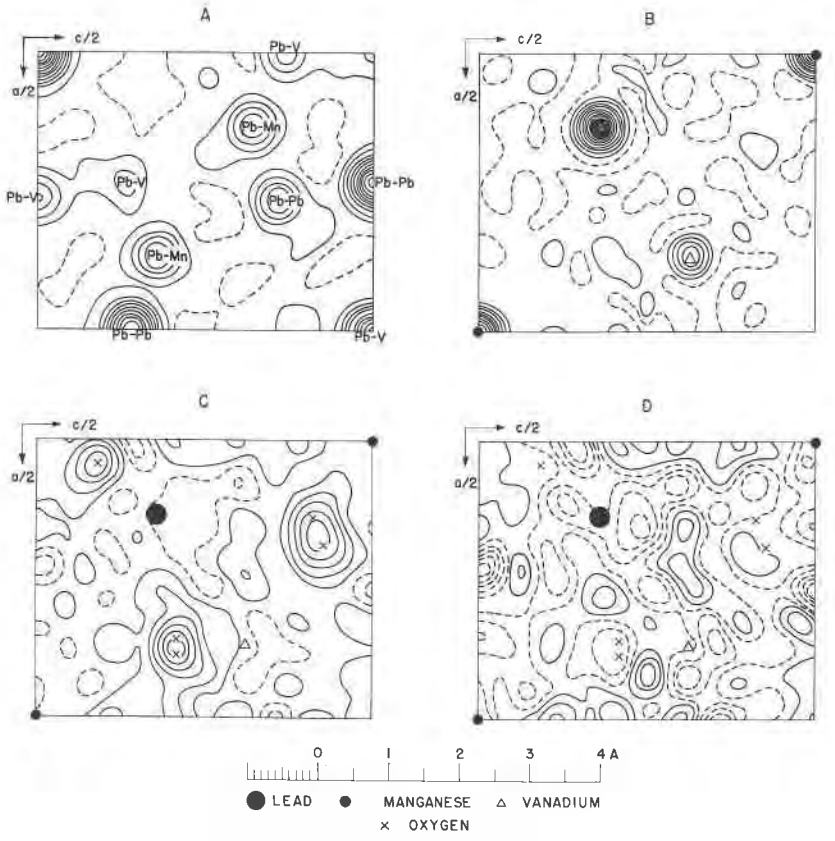

FIG. 1. The $\{h0l\}$ zone of pyrobelonite; (A) Patterson map with contours at regular, but arbitrary, intervals (doubled at origin); (B) Fourier map with contours at intervals of $\sim 5e.\text{Å}^{-2}$ ($10e.\text{Å}^{-2}$ around Pb), zero contour broken; (C) $(F_o - F_{c(m)})$ map with contours at intervals of $\sim 2e.\text{Å}^{-2}$, zero and negative contours broken; (D) final $(F_o - F_c)$ map with contours at intervals of $\sim 1e.\text{Å}^{-2}$, zero and negative contours broken.

The coordinates of the oxygen atoms were obtained, the positions of all the atoms were refined, appropriate temperature factors were determined, and termination-of-series errors were corrected by means of the difference-synthesis technique (Cochran, 1951). Since the accuracy of the results, especially in the location of the oxygen atoms, is dependent on the difference syntheses, it was necessary to exercise care in the selection of values for the atomic scattering factors. The scattering curves for the different atoms were obtained as follows.

Lead. It was assumed that lead is present as the divalent ion. The *atomic* scattering curve for Pb in the *International Tables* (1935), there-

fore, was adjusted to that of Pb^{+2} by reducing the value at $\sin\theta/\lambda=0$ from 82 to 80, leaving those at $\sin\theta/\lambda\geqq 0.4$ unchanged, and drawing a smooth curve from 80 at $\sin\theta/\lambda=0$ to join that representing these higher values.

Manganese. The assumption was made that manganese also is present as the divalent ion. The scattering curve for Mn^{+2} was derived from that of Mn by comparison with those for Ca and Ca^{+2} (*International Tables*, 1935).

Vanadium. It is probable that the vanadium-oxygen bonds have some covalent character and, hence, that vanadium is not present as V^{+5}. Consequently $V^{+2.5}$ was chosen as a compromise between the unionized and fully ionized metalloid atom. The corresponding scattering curve was calculated from recent atomic scattering data for vanadium (Qurashi, 1954) by deducting the contributions of one 4*s* and one and one-half 3*d* electrons, utilizing the screening parameters and individual electron contributions given by Viervoll & Ögrim (1949).

Oxygen. In order to balance the ionic charges present, it was necessary to consider each oxygen atom to have gained $1\frac{1}{2}$ electrons. The scattering curve for $O^{-1.5}$ was obtained by interpolation between the data for O and O^{-2} (*International Tables*, 1935), and was employed for all the oxygen atoms including that of the OH group.

With the foregoing scattering factors for Pb^{+2}, Mn^{+2}, $V^{+2.5}$, corrected for thermal motion, $(F_o-F_{c(m)})$ syntheses were performed, where $F_{c(m)}$ is the structure factor calculated for the metal atoms alone. The map representing the final synthesis of this type is shown in Fig. 1C, where it will be observed that the oxygen atoms appear clearly, although only one of the five in the asymmetric unit is resolved. Nevertheless, x and z coordinates for the oxygen atoms, and some alterations of the metal-atom positions, were obtained from this synthesis.

Refinement of all positions (metal and oxygen atoms), and of the temperature factor corrections, was completed through successive (F_o-F_c) syntheses, where F_c is the structure factor calculated for the metal atoms and the oxygen atoms. The last difference map is reproduced in Fig. 1D, from which it can be seen that the gradients at all the atomic positions are small enough to be neglected. The background density varies from $-4e.Å^{-2}$ to $+4e.Å^{-2}$. The final x, z coordinates obtained for this zone are presented later in Table 4.

The temperature factor corrections, of the usual form $\exp[-B(\sin\theta/\lambda)^2]$, applied to the scattering curves were obtained qualitatively from the difference syntheses by attempting to reduce the background density around the atoms to zero. The final values of B for the $\{h0l\}$ zone are presented later, with those for the other two zones, in Table 5. The struc-

ture factor data, derived from the x, z coordinates of Table 4 (see under $\{h0l\}$), the scattering curves defined previously, and these temperature factors, are given in Table 1. The value of the reliability index R is 0.15 when the metal atoms only are considered, but drops to 0.09 when the contributions of the oxygen atoms are included.

TABLE 1. STRUCTURE FACTOR DATA FOR THE $\{h0l\}$ ZONE (F_o, OBSERVED; $F_{c(m)}$, CALCULATED FOR METAL ATOMS ONLY; F_c, CALCULATED FOR METAL ATOMS AND OXYGEN ATOMS)

hkl	$F_{c(m)}$	F_o	F_c	*hkl*	$F_{c(m)}$	F_o	F_c
000	+520	—	+684	2.0.10	+29	39	+36
200	+44	51	+43	2.0.11	+43	67	+63
400	−218	225	−257	2.0.12	+20	<33	+22
600	+112	139	+125	2.0.13	−83	89	−99
800	+188	184	+194	2.0.14	+33	<36	+29
10.0.0	−38	35	−43	301	−179	127	−125
002	−146	148	−151	302	−91	121	−116
004	+5	<17	−4	303	+166	151	+150
006	+281	234	+243	304	+99	106	+109
008	−146	186	−172	305	−214	215	−222
0.0.10	+76	103	+99	306	−30	49	−48
0.0.12	+107	101	+109	307	−38	83	−72
0.0.14	−80	76	−65	308	−44	27	−30
0.0.16	+74	69	+65	309	+69	84	+75
101	+21	<11	+6	3.0.10	+64	63	+63
102	−133	115	−121	3.0.11	−141	125	−131
103	−291	231	−271	3.0.12	−34	43	−33
104	+138	185	+190	3.0.13	+17	<35	+24
105	+88	76	+63	401	+31	37	+33
106	−40	48	−53	402	+228	226	+251
107	−50	36	−32	403	−4	<21	+2
108	−59	62	−54	404	+100	86	+91
109	−130	130	−134	405	−21	<24	−13
1.0.10	+85	81	+71	406	−142	136	−139
1.0.11	+65	77	+69	407	+25	27	+31
1.0.12	−44	39	−50	408	+193	186	+203
1.0.13	−62	57	−60	409	−10	<30	−12
1.0.14	−15	<36	−9	4.0.10	−5	<31	−20
201	−189	152	−167	4.0.11	−9	<32	−16
202	+96	95	+91	4.0.12	−42	41	−33
203	+30	59	−45	4.0.13	+15	<35	+8
204	+68	77	+62	4.0.14	+112	105	+103
205	+123	118	+112	501	−105	123	−105
206	+28	<23	+27	502	+111	92	+93
207	+145	148	−128	503	+66	59	+50
208	+59	85	+64	504	−121	147	−154
209	+57	73	+60	505	−123	114	−111

TABLE 1—(*continued*)

hkl	$F_{c(m)}$	F_o	F_c	*hkl*	$F_{c(m)}$	F_o	F_c
506	+36	32	+50	804	+3	<30	+8
507	−34	33	−40	805	+28	<31	+25
508	+56	70	+63	806	+145	147	+149
509	+25	31	+38	807	−35	<32	−28
5.0.10	−84	70	−70	808	−76	94	−76
5.0.11	−87	87	−85	809	+14	<35	+22
5.0.12	+43	35	+41	8.0.10	+48	70	+59
601	+123	98	+101	901	−11	31	−16
602	+2	<25	+8	902	−74	79	−81
603	−22	<26	−19	903	−73	72	−67
604	+27	<26	+23	904	+84	73	+85
605	−84	100	−93	905	+4	<33	+2
606	+84	75	+75	906	−26	<34	−35
607	+104	116	+100	907	−26	<34	−19
608	−11	<31	−17	908	−42	<35	−37
609	−44	<32	−31	909	−47	65	−53
6.0.10	+38	56	+38	9.0.10	+64	56	+65
6.0.11	−33	<35	−39	10.0.1	−68	69	−63
6.0.12	+42	<36	+46	10.0.2	+68	69	+66
701	+37	<27	+28	10.0.3	+12	<34	+4
702	+43	49	+44	10.0.4	+38	51	+44
703	−198	175	−189	10.0.5	+48	<35	+50
704	−47	51	−55	10.0.6	−25	<35	−19
705	+85	101	+84	10.0.7	−62	47	−55
706	+16	<30	+30	10.0.8	+66	66	+64
707	−35	<31	−24	11.0.1	−71	72	−75
708	+23	<32	+23	11.0.2	−14	<35	−16
709	−115	121	−124	11.0.3	+80	77	+76
7.0.10	−35	35	−33	11.0.4	+16	<36	+20
7.0.11	+71	70	+65	11.0.5	−101	88	−94
801	−38	48	−44	12.0.2	+70	74	+70
802	−60	80	−74	13.0.2	+45	46	+44
803	+6	<30	−5				

The {0kl} Zone

Of 37 possible reflections in the range sin $\theta/\lambda \leqq 0.6$, 33 were observed. The (100) Patterson map, computed with these terms, is reproduced in Fig. 2A. Examination of this map shows that the peak distributions for the Pb-Pb, Pb-V, and Pb-Mn vectors can be explained satisfactorily if the Pb and V atoms are lying along $y = \pm\frac{1}{4}$ (special positions (c) of *Pnma*) and the Mn atoms are in special positions (b) of *Pnma*. On this basis the space group *Pnma* was adopted provisionally and refinement proceeded by means of Fourier and difference-synthesis techniques as for the {*h*0*l*} zone.

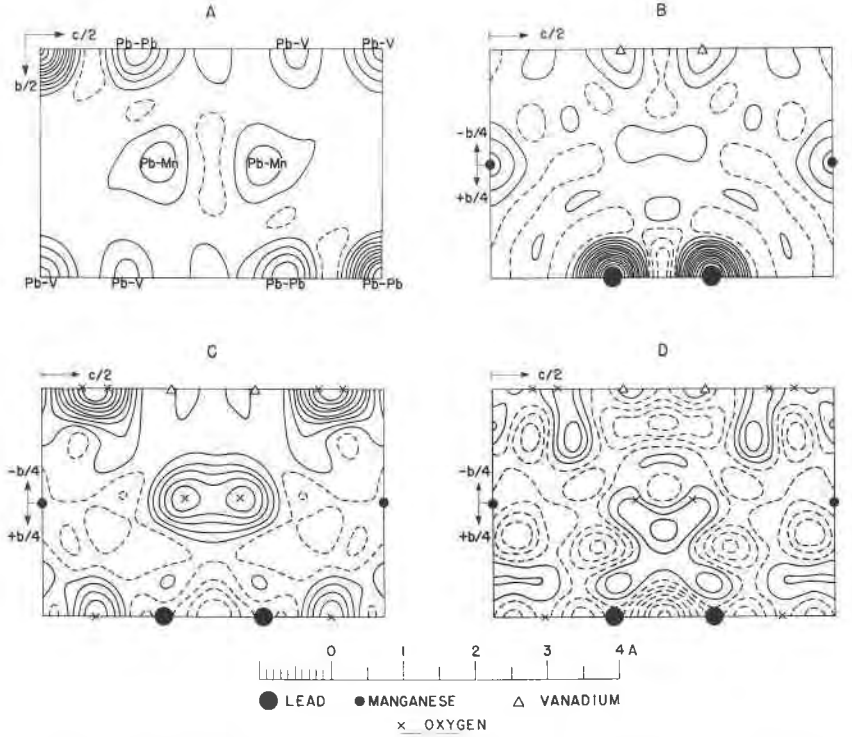

FIG. 2. The $\{0kl\}$ zone of pyrobelonite; (A) Patterson map with contours at regular, but arbitrary, intervals; (B) Fourier map with contours at intervals of $\sim 7e.\text{Å}^{-2}$, zero contour broken; (C) $(F_o - F_{c(m)})$ map with contours at intervals of $\sim 2e.\text{Å}^{-2}$, zero and negative contours broken; (D) final $(F_o - F_c)$ map with contours at intervals of $\sim 1e.\text{Å}^{-2}$, zero and negative contours broken.

The (100) Fourier map is shown in Fig. 2B where, again, the metal atoms are clearly resolved but the positions of the oxygen atoms are only vaguely indicated. Fig. 2C shows the results of the $(F_o - F_{c(m)})$ synthesis from which the coordinates of the oxygen atoms were obtained; only one pair of oxygen atoms is not resolved. The final $(F_o - F_c)$ synthesis is reproduced in Fig. 2D. In this map the gradients at the atomic positions are negligible and the general background density varies from $-3.5e.\text{Å}^{-2}$ to $+3.5e.\text{Å}^{-2}$ with the exception of a trough of $-6e.\text{Å}^{-2}$ between two lead atoms. Examination of the electron density in the immediate vicinity of these lead atoms indicates that they may have a slight degree of asymmetric thermal motion, the effect being multiplied at the trough. No correction for this was applied, however, because the individual effects, if real, are no larger than the random peaks. The final y, z coordinates obtained for the $\{0kl\}$ zone are collected in Table 4.

The final values of the temperature factor constant (B) for this zone are given in Table 5. The structure factor data, based on the y, z coordinates of Table 4 (see under $\{0kl\}$) are presented in Table 2. The reliability index R is 0.16 for the metal atoms alone, and 0.10 for all the atoms. The values of F_o for the planes (020) and (040) are very much smaller than the corresponding values of F_c (see Table 2). This is proba-

TABLE 2. STRUCTURE FACTOR DATA FOR THE $\{0kl\}$ ZONE (F_o, OBSERVED; $F_{c(m)}$, CALCULATED FOR METAL ATOMS ONLY; F_c, CALCULATED FOR METAL ATOMS AND OXYGEN ATOMS)

hkl	$F_{c(m)}$	F_o	F_c	*hkl*	$F_{c(m)}$	F_o	F_c
000	+520	—	+684	0.2.10	−7	<38	+3
020	−262	216	−287	031	+165	158	+164
040	+307	276	+376	033	−27	39	−45
060	−146	142	−156	035	−111	122	−115
002	−147	149	−150	037	+132	142	+133
004	+6	<34	+7	039	−53	53	−55
006	+281	239	+244	042	−105	104	−106
008	−146	170	−172	044	−1	<42	−1
0.0.10	+77	109	+92	046	+212	192	+187
011	−201	152	−183	048	−115	145	−134
013	+31	56	+50	051	−124	105	−113
015	+128	145	+137	053	+21	<43	+25
017	−151	161	−151	055	+85	102	+91
019	+58	65	+58	057	−107	94	−106
0.1.11	+46	57	+49	062	+148	124	+119
022	+274	182	+200	064	+69	82	+85
024	+119	166	+154	066	−102	77	−84
026	−162	139	−132	071	+90	76	+93
028	+215	223	+223	073	−16	25	−26

bly due to extinction and the contributions from these two planes were omitted from the difference syntheses. If they are given zero discrepancy, R for all the atoms becomes 0.06.

The $\{hk0\}$ Zone

All 28 possible reflections in the range $\sin\theta/\lambda \leqq 0.06$ were observed. The (001) Patterson map is reproduced in Fig. 3A. The coordinates obtained from an analysis of this map in terms of the Pb-Pb, Pb-Mn, and Pb-V vectors required no departure from the space group *Pnma*. Refinement, therefore, was carried out as for the previous two zones.

The (001) electron-density map is shown in Fig. 3B. In this zone the lead and vanadium atoms are not resolved and thus were assumed to be exactly superimposed. Good resolution of the manganese atom is ap-

parent but there are no indications of the oxygen atoms. The latter, however, emerge clearly in the $(F_o - F_{c(m)})$ map reproduced in Fig. 3C, with the exception of the OH group. The final $(F_o - F_c)$ synthesis is repre-

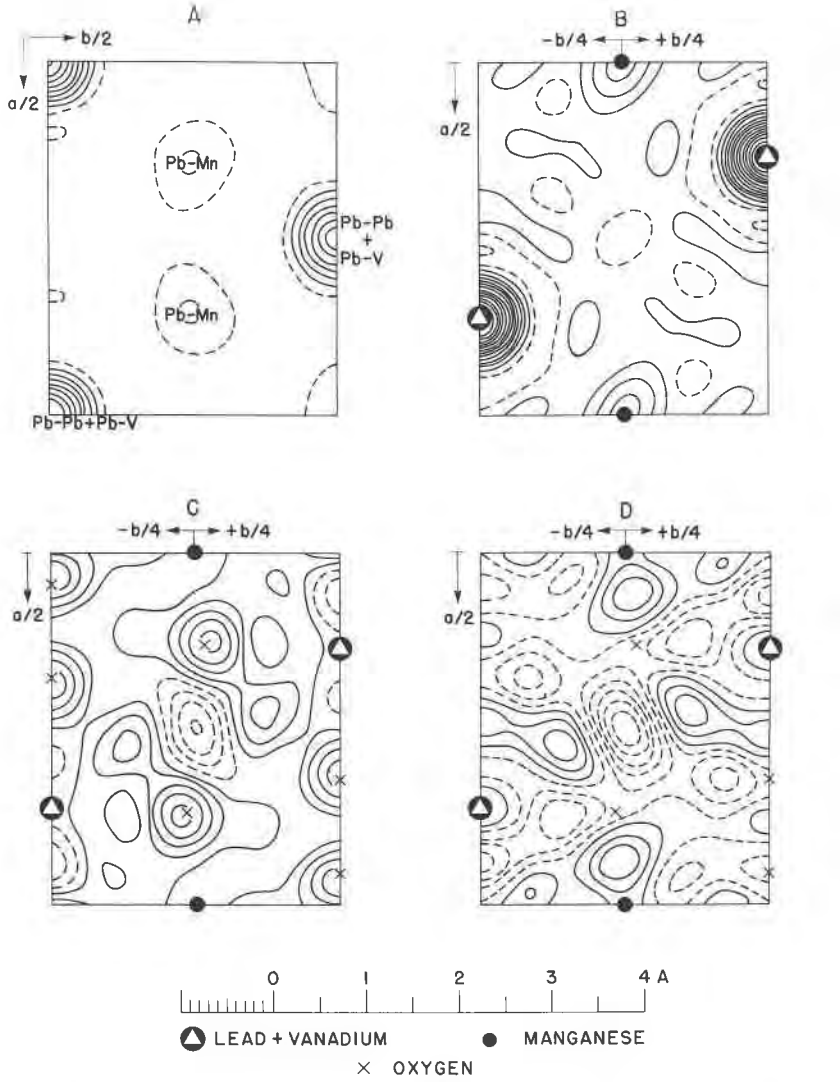

FIG 3. The $\{hk0\}$ zone of pyrobelonite; (A) Patterson map with contours at regular, but arbitrary, intervals; (B) Fourier map with contours at intervals of $\sim 7e.\text{Å}^{-2}$, zero contour broken; (C) $(F_o - F_{c(m)})$ map with contours at intervals of $\sim 2e.\text{Å}^{-2}$, zero and negative contours broken; (D) final $(F_o - F_c)$ map with contours at intervals of $\sim 1e.\text{Å}^{-2}$, zero and negative contours broken.

sented in Fig. 3D, where the gradients at the atomic positions are negligibly small and, apart from a trough of $-6e.\text{Å}^{-2}$ at $(\frac{1}{4},0)$, the general background density varies from $-3.5e.\text{Å}^{-2}$ to $+3.5e.\text{Å}^{-2}$. Although there are indications in this case of possible asymmetric thermal motion of the manganese atoms no corrections for this were applied because the variation in electron density around the manganese atoms is of the same order of magnitude as the general background.

In the projection of this zone, the lead and vanadium atoms appear to be exactly superimposed; if they are not, the separation can only be very slight because no shifts from the superimposed positions were indicated by the difference syntheses (Fig. 3D). The reason for the apparent absence of the hydroxyl group can be found by reference to the x, y coordinates obtained for the $\{h0l\}$ and $\{0kl\}$ zones (Table 4); the OH is present in the large peak representing the lead and vanadium atoms. With this information, an adjustment of the temperature factor corrections could have been applied to the scattering curves for these two atoms in order to produce a peak for the OH group in the difference syntheses of the $\{hk0\}$ zone. This would have vitiated the complete independence of treatment of this zone, however, and therefore no allowance for the OH group was made during the refinement procedure.

The final x, y coordinates obtained for the $\{hk0\}$ zone are given in Table 4.

The final values of the temperature factor constant (B) for this zone are listed in Table 5. The structure factor data, calculated with the x y, coordinates of Table 4 (see under $\{hk0\}$) are given in Table 3. The reliability index R is 0.12 for the metal atoms only and 0.08 when the oxygen atom contributions are included. The values of F_o for (020), (040), and (210) are very much smaller than the corresponding values of F_c (see Table 3). This again is probably due to extinction and the contributions from these three planes were omitted from the difference syntheses. If they are given zero discrepancy, R for all the atoms becomes 0.04.

Correlation of the Results from the Three Zones

Although the reflection intensities for each zone were placed on an approximately absolute scale independently of the data for the other two zones, the differences in scale from zone to zone are very small as may be seen by a comparison of F_o's for the axial reflections common to pairs of zones (Tables 1, 2, 3). In fact the difference in scale of the $00l$ reflections (common to the $\{h0l\}$ and $\{0kl\}$ zones), calculated from

$$\frac{\Sigma F_{00l}(\text{ for } \{h0l\}) - \Sigma F_{00l}(\text{for } \{0kl\})}{\frac{1}{2}[\Sigma F_{00l}(\text{for } \{h0l\}) + \Sigma F_{00l}(\text{for } \{0kl\})]}$$

TABLE 3. STRUCTURE FACTOR DATA FOR THE $\{hk0\}$ ZONE (F_o, OBSERVED; $F_{c(m)}$, CALCULATED FOR METAL ATOMS ONLY; F_c, CALCULATED FOR METAL AND OXYGEN ATOMS)

hkl	$F_{c(m)}$	F_o	F_c	*hkl*	$F_{c(m)}$	F_o	F_c
000	+520	—	+684	410	+68	74	+66
200	+36	45	+38	420	+304	264	+270
400	−208	225	−236	430	−57	53	−54
600	+124	136	+142	440	−151	180	−166
800	+172	183	+177	450	+43	43	+43
020	−259	220	−260	460	+176	161	+161
040	+301	296	+355	610	+193	201	+211
060	−132	137	−135	620	−30	36	−34
210	−337	254	−309	630	−167	190	−176
220	+109	118	+99	640	+97	112	+110
230	+270	240	+240	650	+132	150	+149
240	+22	35	+23	810	−74	66	−62
250	−195	191	−191	820	−94	85	−70
260	+58	69	+55	830	+67	61	+58
270	+136	115	+118				

is less than 1%; it is 2% for the $h00$ reflections (common to the $\{h0l\}$ and $\{hk0\}$ zones), and it is 3% for the $0k0$ reflections (common to the $\{hk0\}$ and $\{0kl\}$ zones). Furthermore, the discrepancies between the F_o's for the set of axial reflections common to a pair of zones, calculated from expressions of the form

$$\frac{\Sigma|F_{00l}(\text{for }\{h0l\}) - F_{00l}(\text{for }\{0kl\})|}{\frac{1}{2}[\Sigma F_{00l}(\text{for }\{h0l\}) + \Sigma F_{00l}(\text{for }\{0kl\})]}$$

lie between 2% and 5% for the three pairs of principal zones. Since this is the order of accuracy to be expected of F_o's obtained from visually estimated intensities, the errors in the absorption corrections, as anticipated, must be small.

The atomic coordinates obtained independently for each zone together with the mean values are listed in Table 4. In all cases, the average is the arithmetic mean except for O(3) and O(4).

The maximum difference between two values of the same coordinate for the lead atoms occurs for x (see Table 4) and corresponds to 0.014 Å. The discrepancy probably is attributable to the value for the $\{hk0\}$ zone because V is superimposed on Pb in the (001) maps (Fig. 3). Because the discrepancy is so small, however, the values were not weighted in calculating the mean. No similar assessment of the manganese coordinates is possible because of their special positions. The largest difference in the vanadium coordinates (x) corresponds to 0.006 Å.

The differences between values for the same oxygen coordinates vary

TABLE 4. FRACTIONAL COORDINATES OF THE ATOMS (DERIVED INDEPENDENTLY FOR EACH ZONE AND THEN AVERAGED)

Atom	x			y			z		
	$\{hk0\}$	$\{h0l\}$	Mean	$\{hk0\}$	$\{0kl\}$	Mean	$\{h0l\}$	$\{0kl\}$	Mean
Pb	0.1350	0.1332	0.1341	1/4	1/4	1/4	0.1776	0.1775	0.1776
Mn	0	0	0	0	0	0	1/2	1/2	1/2
V	0.3650	0.3658	0.3654	3/4	3/4	3/4	0.3130	0.3125	0.3128
O(1)	0.178	0.190	0.184	3/4	3/4	3/4	0.432	0.442	0.437
O(2)	0.538	0.542	0.540	3/4	3/4	3/4	0.410	0.405	0.408
O(3)	0.367	0.360	0.371	0.515	0.510	0.513	0.207	0.210	0.209
O(4)	0.367	0.390	0.371	0.985	0.990	0.987	0.207	0.210	0.209
OH	—	0.139	0.139	—	1/4	1/4	0.412	0.422	0.417

from 0.029 to 0.095 Å with the exception of one of 0.176 Å (see fractional coordinates x for O(4), Table 4), but, even with the inclusion of this one, the r.m.s. difference is only 0.078 Å. If the space group is *Pnma* (and not *Pn2a*), O(3) and O(4) must be superimposed exactly in the (010) projection by virtue of the mirror plane perpendicular to *b*. In Fig. 1C, O(3) and O(4) are not separately resolved, but, in the final difference map (Fig. 1D) there is some evidence that they may not have precisely the same x coordinate; this is recognized by the inclusion of $x=0.360$ for O(3) and $x=0.390$ for O(4) in the appropriate $\{h0l\}$-column of Table 4. In view of the fact that this is the sole indication that *Pnma* might not be the correct choice of space group, and that it depends on a single coordinate of an unresolved oxygen atom, it cannot be given very much weight. It is still possible, of course, that some deviations from the special positions of *Pnma* have not been found (and hence that the space group is really *Pn2a*) but they would have to be very small in the case of the metal atoms, although they could be larger for the atoms of oxygen (see the standard deviations of atom-positions given later). Therefore, the space group *Pnma* has been retained and the final (mean) values of the coordinates of O(3) and O(4) are the averages of those for *both* atoms (see Table 4).

The corrections applied to the atomic scattering curves for isotropic thermal motion of the atoms are collected in Table 5. The variation

TABLE 5. VALUES OF THE TEMPERATURE FACTOR CONSTANT, B, FOR EACH OF THE THREE ZONES

Atom	$\{hk0\}$	$\{0kl\}$	$\{h0l\}$
Pb	1.2	0.9	0.9
Mn	0.5	0.7	0.7
V	1.0	0.7	0.8
O	0	0	0

among the factors for the same atom in each of the three zones is small, thus indicating very little, if any, asymmetric component. This is borne out by the final difference maps (see Figs. 1D, 2D, 3D).

Accuracy of Results

Standard deviations of peak positions were calculated from $\sigma(x) = \sigma(A_h)/A_{hh}$, where

$$\sigma(A_h) = \frac{2\pi}{aA}(\Sigma h^2 \Delta F^2)^{1/2}$$

and A_{hh} is the curvature at these points on the electron-density maps (Cruickshank, 1949). If the curve at the peak position of a resolved atom is represented by the expression $\rho = a + br + cr^2$, then $A_{hh} = \delta^2\rho/\delta r^2) = 2c$. Assuming the peaks to be spherically symmetrical (reasonably justified by Figs. 1D, 2D, 3D), and hence that $\sigma(x) \simeq \sigma(y) \simeq \sigma(z) = \sigma$, the standard deviations (σ) in their positions are 0.01 Å for lead, 0.04 Å for vanadium, 0.05 Å for manganese, and 0.11 Å for oxygen, the curvatures at the oxygen positions, of necessity, being obtained from the partial difference maps (Figs. 1C, 2C, 3C), while those for the metal atoms were taken from the Fourier maps (Figs. 1B, 2B, 3B). The values for these standard deviations are supported by the good agreement between the same coordinates measured separately in two zones (see Table 4), for which the

Table 6. Standard Deviations (in Å) of Interatomic Distances

Pb-O,	0.11	Pb-Pb,	0.014	Mn-Mn,	0.07
Mn-O,	0.12	Pb-Mn,	0.05	Mn-V,	0.06
V-O,	0.12	Pb-V,	0.04	V-V,	0.06
O-O,	0.16				

r.m.s. deviations are 0.01 Å for lead, 0.006 Å for vanadium, and 0.078 Å for oxygen. It thus appears, on the basis of $\sigma = 0.11$ Å for the oxygen positions, that the relatively large difference of 0.176 Å for the x-coordinate of O(4), obtained from the data for the $\{hk0\}$ and $\{h0l\}$ zones (Table 4), should not be considered as significant (Cruickshank, 1949, p. 67).

Standard deviations of interatomic distances were calculated with expressions of the form $\sigma_{Pb-V} = [\sigma_{Pb}^2 + \sigma_V^2]^{\frac{1}{2}}$ and are collected in Table 6.

Description of the Structure and Interatomic Distances

The coordination of oxygen atoms around the atoms of vanadium is tetrahedral, with V at distances of 1.83 Å from O(1), 1.62 Å from O(2), and 1.77 Å from O(3) and from O(4). The six closest oxygen-oxygen distances in this tetrahedron lie in the range 2.72–2.99 Å. On the basis of

the standard deviations of interatomic distances, the VO_4 tetrahedron is regular within the limits of experimental error.

There is a tetragonal bipyramidal arrangement of oxygen atoms around the atoms of manganese, with Mn-O distances of 2.04, 2.18, and 2.22 Å (three values only, because Mn is at a centre of symmetry). The twelve closest oxygen-oxygen distances in this polyhedron vary from 3.09 to 3.14 Å, and thus, on the basis of the standard deviations for Mn-O and O-O (see Table 4), the oxygen atoms form a regular octahedron with Mn at the centre, within the limits of experimental error.

The coordination of oxygen atoms around Pb is less regular. Each atom of lead has seven nearest oxygen neighbours, the Pb-O distances varying from 2.28 to 2.89 Å. There must, therefore, be real differences among the Pb-O distances because some of these differences are greater than three times the standard deviation of 0.11 Å (Cruickshank, 1949, p. 67).

The closest approach of lead atoms is 4.07 Å (between Pb at $x, \frac{1}{4}, z$ and Pb at $\frac{1}{2}+x, \frac{1}{4}, \frac{1}{2}-z$), that of manganese atoms is 3.10 Å ($=b/2$), and that of vanadium atoms is 4.11 Å (between V at $x, \frac{3}{4}, z$ and V at $\frac{1}{2}+x, \frac{3}{4}, \frac{1}{2}-z$). The shortest Pb-Mn distances are 3.59 Å between Pb at x, y, z and Mn at 0, 0, $\frac{1}{2}$, and 3.62 Å between Pb at x, y, z and Mn at $\frac{1}{2}$, 0, 0. Between lead and vanadium, the closest approach is 3.47 Å (between Pb at $\frac{1}{2}-x, \frac{3}{4}, \frac{1}{2}+z$ and V at $x, \frac{3}{4}, z$), with the next nearest lead atoms at distances of 3.72 Å (for Pb at $\frac{1}{2}+x, \frac{1}{4}, \frac{1}{2}-z$) and 3.79 Å (for Pb at x,y,z), respectively, from the same vanadium atom. The shortest distance between manganese and vanadium is 3.51 Å (Mn at 0, 0, $\frac{1}{2}$; V at $\frac{1}{2}-x, \frac{1}{4}, \frac{1}{2}+z$).

Discussion

The structure of pyrobelonite is almost identical with that of descloizite (Qurashi & Barnes, 1954), as was anticipated from the close correspondence, both in relative intensities and in Bragg angles, of reflections from the three principal zones of each. The main differences are in the locations of the oxygen atoms which, in pyrobelonite, deviate appreciably from the idealized positions assigned provisionally to them in the descloizite structure (cf. Figs. 1C, 2C, 3C with Fig. 3 of Qurashi & Barnes, 1954). No special significance should be attached to this, however, until refinement of the descloizite structure is complete. A better comparison is afforded between the present Figs. 1C, 2C, 3C and the corresponding partial difference maps for conichalcite (Qurashi & Barnes, 1954, Fig. 8), from which it will be observed that agreement between corresponding oxygen-atom positions is very good.

The difference between the density (5.79 gm. per ml.) calculated on the basis of $4[PbMn(VO_4)(OH)]$ per unit cell and the measured values

of 5.377 (Flink, 1919) and 5.58 (this paper), both for Långban material, is somewhat puzzling. The lower value (5.377) implies a Mn:Pb ratio of ~32:22 (close to that of the Mauzelius analysis; Flink, 1919), but, assuming random substitution of Mn for Pb throughout the lattice this would reduce the observed peak heights for Pb by almost 20%. There was no evidence of any such effect in the present structure analysis. It seems probable, therefore, that the earlier density measurement is much too low. The present value of 5.58 gm. per ml. (obtained with the only suitable crystal available and, as mentioned previously, also probably low) corresponds to a Mn:Pb ratio of ~27:22. It is, of course, possible that substitution may exist to varying degrees in different specimens even from the same locality, but, certainly in the two crystals employed for the present structure investigation, any substitution of part of the lead by manganese could only be negligibly small. It is highly desirable that the density of pyrobelonite should be redetermined if suitable specimens can be found.

Acknowledgments

Grateful acknowledgement is made to Professor Clifford Frondel for the crystals of pyrobelonite employed for the structure determination and the density measurement, to Dr. George Switzer for crystals from a U. S. National Museum specimen which it was hoped could be ground into spheres for more precise absorption corrections, and to Mrs. M. E. Pippy for assistance with the calculations.

References

Barnes, W. H. & Qurashi, M. M. (1952): Unit cell and space group data for certain vanadium minerals, *Am. Mineral.*, **37**, 407–422.

Berman, H. (1939): A torsion microbalance for the determination of specific gravities of minerals, *Am. Mineral.*, **24**, 434–440.

Bradley, A. J. (1935): The absorption factor for the powder and rotating-crystal methods of *x*-ray crystal analysis, *Proc. Phys. Soc.*, **47**, 879–899.

Cochran, W. (1951): The structures of pyrimidines and purines. V. The electron distribution in adenine hydrochloride, *Acta Cryst.*, **4**, 81–92; Some properties of the $(F_o - F_c)$-synthesis, *Acta Cryst.*, **4**, 408–411.

Cruickshank, D. W. J. (1949): The accuracy of electron-density maps in *x*-ray analysis with special reference to dibenzyl, *Acta Cryst.*, **2**, 65–82.

Dana, J. D. & E. S. (1951): *System of Mineralogy*, **2**, ed. 7, by C. Palache, H. Berman and C. Frondel, New York, p. 816.

Evans, H. T., & Ekstein, M. G. (1952): Tables of absorption factors for spherical crystals, *Acta Cryst.*, **5**, 540–542.

Fairbairn, H. W., & Sheppard, C. W. (1945): Maximum error in some mineralogic computations, *Am. Mineral.*, **30**, 673–703.

Flink, G. (1919): *Geol. Fören. Förh.*, **41**, 433, reference obtained from Hintze (1933), Strunz (1939), Richmond (1940), Dana (1951), *loc. cit.*

HINTZE, C. (1933): *Handbuch der Mineralogie*, Bd. 1, Abt. 4, Berlin, pp. 673–675.

International Tables for the Determination of Crystal Structures (1935), Berlin.

QURASHI, M. M. (1954): On the completion and extension of the table of atomic scattering factors published by Viervoll and Ögrim, *Acta Cryst.*, **7**, 310–312.

QURASHI, M. M., & BARNES, W. H. (1954): The structures of the minerals of the descloizite and adelite groups: I—descloizite and conichalcite (part 1), *Am. Mineral.*, **39**, 416–435.

RICHMOND, W. E. (1940): Crystal chemistry of the phosphates, arsenates, and vanadates of the type $A_2XO_4(Z)$, *Am. Mineral.*, **25**, 441–479.

STRUNZ, H. (1939): Mineralien der Descloizitgruppe, *Zeit. Krist.*, (A) **101**, 496–506.

VIERVOLL, H., & ÖGRIM, O. (1949): An extended table of atomic scattering factors, *Acta Cryst.*, **2**, 277–279.